J. Math. Biol. (2012) 64:981–1004
DOI 10.1007/s00285-011-0441-5

Mathematical Biology

Time optimal control of spiking neurons

Ali Nabi · Jeff Moehlis

Received: 13 September 2010 / Revised: 8 April 2011 / Published online: 10 June 2011

Abstract By injecting an electrical current control stimulus into a neuron, one can change its inter-spike intervals. In this paper, we investigate the time optimal control problem for periodically firing neurons, represented by different one-dimensional phase models, and find analytical expressions for the minimum and maximum values of inter-spike intervals achievable with small bounded control stimuli. We consider two cases: with a charge-balance constraint on the input, and without it. The analytical calculations are supported with numerical results for examples of qualitatively different neuron models.

Keywords Time-optimal control · Mathematical neuroscience · Phase models

Mathematics Subject Classification (2000) 34H05 · 49J15 · 49J30 · 93C15

1 Introduction

Oscillatory neurons periodically emit action potentials in the form of voltage spikes. Various mathematical models have been developed to capture the essentials of such oscillatory behavior (Hodgkin and Huxley 1952; Keener and Sneyd 1998; Rose and Hindmarsh 1989; Rinzel and Ermentrout 1998; Izhikevich 2007). A powerful

---

This work was supported by the National Science Foundation Grant NSF-0547606 and 1000678.

A. Nabi (✉) · J. Moehlis
Mechanical Engineering Department, University of California at Santa Barbara,
Santa Barbara, CA 93106, USA
e-mail: nabi@engineering.ucsb.edu

J. Moehlis
e-mail: moehlis@engineering.ucsb.edu

technique for analyzing these mathematical models is phase reduction, in which the multi-dimensional model is reduced to a one-dimensional phase model. Here the oscillatory behavior of the neuron is represented by the evolution of this single phase variable (Kuramoto 1984; Brown et al. 2004b; Izhikevich 2007). Phase models of neurons have been used to investigate the patterns of synchrony that result from the type and architecture of coupling (Brown et al. 2003; Ghigliazza and Holmes 2004; Cohen et al. 1982; Kopell and Ermentrout 1990; Ashwin and Swift 1992; Hansel et al. 1993; Gerstner et al. 1996), and the response of large groups of oscillators to external stimuli (Brown et al. 2004a,b; Tass 1999; Forger and Paydarfar 2004).

Phase models of neurons have also been employed in the context of controlling neurons to give a prespecified behavior (Tass 1999; Moehlis et al. 2006; Danzl et al. 2010; Nabi and Moehlis 2010). Much of the motivation for controlling neurons comes from the desire to treat certain neurological diseases such as epilepsy and Parkinson's disease. In Parkinson's disease, for instance, the patient experiences involuntary tremors that have been associated with the synchronization of a cluster of neurons in the thalamus and basal ganglia (Pare et al. 1990). For a surgical treatment referred to as electrical deep brain stimulation (EDBS), a neurosurgeon guides a small electrode into the motor-control region of the brain through which high-frequency ($\geq$100 Hz) electrical current pulses are sent directly into the brain tissue, which empirically has been found to reduce tremors for some patients (Benabid et al. 1991).

An area of recent research interest has been to find control stimuli, in the form of electrical currents, that can effectively break this pathological synchrony; see, for example, Tass (1999) and Danzl et al. (2009). On a single neuron level, this objective reduces to controlling the spiking time of a single neuron. Here, upon detection of a voltage spike (or a firing event), a precomputed input stimulus is injected into the neural system that would shift the next spike time to a certain prespecified value. This input stimulus may be computed under different criteria and/or constraints. For example in Moehlis et al. (2006), the control law which minimizes the input energy is calculated.

In this paper, we instead investigate the *time optimal* control for a single neuron described by a phase model, and in particular find the extreme values of the next firing time when the input is constrained between some prespecified upper and lower bounds. In such time optimal control problems, which give what is known as bang-bang control, the objective is to find an input that would take the system to the target point in minimum or maximum time, without a constraint on the amount of energy needed. From this analysis, one can gain insight about the maximum capability of treatment procedures like deep brain stimulation when input stimuli are bounded. The main focus here will be on charge-balanced input stimuli, a nontrival extension of the time optimal control calculations in Moehlis et al. (2006) which did not require charge-balance. The analysis also differs from the work in Nabi and Moehlis (2009) and Danzl et al. (2010), which considered *energy optimal* control with a charge-balance constraint.

The charge-balance constraint ensures that the total electrical charge that is transferred to the neural tissue is zero over the course of one cycle of control input. This is important to prevent neural tissue damage. Applying charge-imbalanced inputs, especially uni-sign inputs, to the neuron causes irreversible Faradaic chemical reactions to take place in the environment immediate to the electrode, which results in permanent damage to the tissue. With charge-balanced inputs, one prevents this damage, although this is likely to cause corrosive damage to the electrode, something that can be mitigated by modifying the material and design of the electrode (Merrill et al. 2005).

There may be other applications of deep brain stimulation for which the results presented in this paper are relevant, in particular treatments of disorders for which the increase in the neurons' firing rate is desireable; this might also be useful for enhancing a person's performance, for example by heightening their attention through targeted stimulation. The results might also be relevant for other stimulated oscillators for which a phase reduction can be performed. In the biological context, this could include the heart as stimulated by an artificial pacemaker, or an organisim's circadian rhythm as stimulated by light or chemicals (Forger and Paydarfar 2004; Revell 2005; Shaik et al. 2008).

The organization of this paper is as follows. In Sect. 2, we first introduce the dynamic phase equation and then we develop and provide solution to the time optimal control problem formulation in its general format. In Sect. 3, we present four different neural models and solve the control problem for each of these models. We give detailed analytical results for three of these models, and numerical results for all four. We summarize and discuss the results in Sect. 4.

2 Model equations

A periodically firing or spiking neuron can be considered to be a periodic oscillator with the general dynamical equation (Winfree 2001; Moehlis et al. 2006; Brown et al. 2004b)

$$\frac{d\theta}{dt} = f(\theta) + Z(\theta)u(t). \tag{1}$$

This equation is referred to as the phase model for the neuron. Here, $f(\theta)$ represents the neuron's baseline dynamics, $Z(\theta)$ is called the Phase Response Curve (PRC) of the neuron, and $u(t)$ is the control input which is an electrical current divided by the capacitance of the neural membrane (Moehlis et al. 2006; Brown et al. 2004b). $\theta(t) \in \mathbb{R}^{\geq 0}$, is the neuron's phase, where by convention $\{\theta | \theta \ mod \ 2\pi = 0\}$ corresponds to the spiking of the neuron. We note that the typical definition of phase for neurons is such that for realistic neuron models it yields $f(\theta) =$ constant. However, there are models in the literature (like the theta neuron model that we consider later) that have non-constant $f(\theta)$ functions; in the excitable region, where the neuron periodically fires, we have $f(\theta) > 0$. The PRC for a neuron characterizes a measure of how sensitive the phase of the neuron is to external stimuli. The timing of the external input plays an important role in the amount of phase shift in the neuron. It is very unlikely to have a case where the neuron would be insensitive to the time of the input stimulus. This means that the PRC does not usually have a constant flat part.

For intrinsically oscillatory neurons with $u(t) = 0$, the neuron would fire (or spike) at its natural period T, determined by $f(\theta)$. Without loss of generality, we assume that the initial time of firing is $t = 0$. By inputting a control stimulus $u(t)$, the next firing time of the neuron, or the Inter-Spike Interval (ISI), can be adjusted to a desired target time $t_1 \neq T$. However, we note that $|u(t)|$ must be sufficiently small for the phase model to remain valid. Strictly speaking, the phase reduction assumes that $|u(t)|$ is infinitesimal, but in practice (1) is a good model for small inputs. We will only consider inputs which are small enough that $\dot{\theta} > 0$ for all times; we view this as a necessary condition for the validity of the model. As is typical for realistic neuron models, we also assume that $Z(\theta)$ has isolated roots and furthermore, we assume that there does not exist $\tau_1, \tau_2 : 0 \leq \tau_1 < \tau_2 \leq t_1$ such that $Z(\theta(t))f'(\theta(t)) = Z'(\theta(t))f(\theta(t)), \ \forall t \in [\tau_1, \tau_2]$. We use this assumption later in Lemma 1 to prove that a particular function of $Z(\theta)$ that is of interest also has isolated roots. We note that this assumption is valid for most realistic neuron models in the literature.

The objective here is to find the control input $u(t)$ that, when bounded to be less than a certain value $\bar{u}$ in magnitude, i.e. $|u(t)| \leq \bar{u}$, would result in the minimum/maximum value of t_1. This is an optimization problem in which the next spike time t_1 needs to be extremized. This yields $C(t_1) = \int_0^{t_1} 1\, dt$ as the cost function for this system. We will solve this problem for two different cases: with and without a charge-balance constraint imposed on the control input. The charge-balance constraint can be mathematically expressed as $\int_0^{t_1} u(t)dt = 0$. In order to simplify the upcoming calculations, we restate this constraint as follows.

Let $\dot{q} = u(t)$. Integrating both sides of this equation from 0 to t_1, we obtain

$$q(t_1) - q(0) = \int_0^{t_1} u(\tau)d\tau.$$

For the charge-balance constraint to hold we need the righthand side of this equation to be zero. This means $q(t_1) = q(0)$, and assuming that the input is being applied from time $t = 0$, which implies $q(0) = 0$, we have $q(t_1) = q(0) = 0$.

Summarizing, we seek a control input $u(t)$, which extremizes

$$C(t_1) = \int_0^{t_1} 1\, dt,$$

with the following constraints:

$$\begin{aligned} \dot{\theta} &= f(\theta) + Z(\theta)u(t), \quad \theta(0) = 0, \quad \theta(t_1) = 2\pi, \\ \dot{q} &= u(t), \ |u(t)| \leq \bar{u}, \quad q(0) = 0, \quad q(t_1) = 0. \end{aligned} \tag{2}$$

The Hamiltonian associated with this system is

$$H(\theta, q, \lambda_1, \lambda_2, u) = 1 + \lambda_1(f(\theta) + Z(\theta)u(t)) + \lambda_2 u(t), \tag{3}$$

where λ_1 and λ_2 are the Lagrange multipliers or the co-states for this system. To obtain the necessary conditions for optimality one can use the Hamiltonian in (3) and write

$$\dot{\theta} = \frac{\partial H}{\partial \lambda_1} \Rightarrow \dot{\theta} = f(\theta) + Z(\theta)u(t), \tag{4}$$

$$\dot{\lambda}_1 = -\frac{\partial H}{\partial \theta} \Rightarrow \dot{\lambda}_1 = -\lambda_1(f'(\theta) + Z'(\theta)u(t)), \tag{5}$$

$$\dot{q} = \frac{\partial H}{\partial \lambda_2} \Rightarrow \dot{q} = u(t), \tag{6}$$

$$\dot{\lambda}_2 = -\frac{\partial H}{\partial q} \Rightarrow \dot{\lambda}_2 = 0, \tag{7}$$

where prime represents differentiation with respect to θ (Kirk 1970; Lenhart and Workman 2007).

The optimal control for this problem is obtained from Pontryagin's minimum principle (Kirk 1970; Lenhart and Workman 2007) as

$$u^*(t) = \arg \mathcal{M}_{|u(t)|\leq \bar{u}} \left(1 + \lambda_1^* \left(f(\theta^*) + Z(\theta^*)u(t)\right) + \lambda_2^* u(t)\right),$$

where $\mathcal{M} \in \{\min, \max\}$. This yields the following equations for the optimal control input, $u^*(t)$, for the cases of minimizing the ISI (or t_1) of the neuron and maximizing it:

$$u^*(t) = -\text{sign}[\lambda_1^* Z(\theta^*) + \lambda_2^*]\bar{u} \quad \text{for the min. problem,} \tag{8}$$

$$u^*(t) = +\text{sign}[\lambda_1^* Z(\theta^*) + \lambda_2^*]\bar{u} \quad \text{for the max. problem.} \tag{9}$$

The star superscript indicates the optimal trajectories or functions. Equations (8) and (9) indicate that the magnitude of the optimal control is always equal to its bound and that only its sign changes with respect to time. This solution, known as bang-bang control, is expected since the objective here is to achieve extreme final time, and thus one expects maximum effort from the control stimulus. These equations hold because $(\lambda_1 Z(\theta) + \lambda_2)$ only has isolated roots, as follows:

Lemma 1 *Suppose $Z(\theta)$ has isolated roots and that there does not exist $\tau_1, \tau_2 : 0 \leq \tau_1 < \tau_2 \leq t_1$ such that $Z(\theta(t))f'(\theta(t)) = Z'(\theta(t))f(\theta(t)), \ \forall t \in [\tau_1, \tau_2]$. Then, the roots of $\lambda_1 Z(\theta) + \lambda_2$ are isolated.*

Proof By contradiction, assume that $\exists\, \tau_1, \tau_2 : 0 \leq \tau_1 < \tau_2 \leq t_1$ such that $\lambda_1 Z(\theta) + \lambda_2 \equiv 0 \ \forall t \in [\tau_1, \tau_2]$. Taking the derivative of this with respect to time, one gets $\dot{\lambda}_1 Z + \lambda_1 Z' \dot{\theta} \equiv 0$. Substituting for $\dot{\lambda}_1$ from (5) and $\dot{\theta}$ from (4), dividing both sides by λ_1, and simplifying the results, we get $Zf' = Z'f$ which contradicts the prior assumptions. □

Minimizing the ISI corresponds to speeding up the neuron dynamics, whereas maximizing it corresponds to slowing it down. Equations (4)–(7) are ordinary differential equations that need to be solved in order to evaluate the optimal control equations (8) and (9). When solving the system, we have these four ODEs along with one of the last two algebraic equations for $u^*(t)$, depending on which optimization problem is being considered. This makes five equations with six unknowns: $\theta^*(t)$, $\lambda_1^*(t)$, $q^*(t)$, $\lambda_2^*(t)$, $u^*(t)$, and the next spike time t_1. So we need one more equation to be able to solve this problem. This sixth equation is obtained from the fact that in the absence of any end point cost on the states of the system, the final value of the Hamiltonian evaluated along the optimal trajectories needs to be zero, regardless of whether the minimization problem or the maximization problem is considered (Kirk 1970; Lenhart and Workman 2007). This can be stated mathematically as

$$H(\theta^*(t_1), \lambda_1^*(t_1), q^*(t_1), \lambda_2^*(t_1), u^*(t_1)) = 0. \tag{10}$$

Equations (4)–(8)/(9) together with (10) comprise a two point boundary value problem (TPBVP) where the boundary values for $\theta(t)$ and $q(t)$ are given in (2). We note that since (4)–(7) are a Hamiltonian system, (10) holds for all $t \in [0, t_1]$. The total input energy associated with the optimal control can be obtained by

$$E(u^*, t_1) = \int_0^{t_1} [u^*(t)]^2 dt = t_1 \bar{u}^2.$$

In order to solve this problem we substitute (8) and (9) into (4) and (5) to get

$$\dot{\theta} = f(\theta) \mp Z(\theta)\mathrm{sign}[\lambda_1 Z(\theta) + \lambda_2]\bar{u}, \tag{11}$$

$$\dot{\lambda}_1 = -\lambda_1 \left(f'(\theta) \mp Z'(\theta)\mathrm{sign}[\lambda_1 Z(\theta) + \lambda_2]\bar{u}\right), \tag{12}$$

where, here and elsewhere, the top signs are for the minimization problem and the bottom signs are for the maximization problem. In the minimization (resp., maximization) problem, the average angular velocity of the system with external stimulus has to be larger (resp., smaller) than that of the system running without any external stimuli. In other words, when the system is stimulated, $\theta(t)$ goes from zero to 2π in time $t_1 < T$ (resp., $t_1 > T$), where T is the natural period of the system without any stimuli. So if we integrate both the stimulated and the unstimulated systems from $t = 0$ to $t = t_1$, while the stimulated system reaches $\theta(t_1) = 2\pi$, the unstimulated system reaches $\theta(t_1) < 2\pi$ in the minimization problem and $\theta(t_1) > 2\pi$ in the maximization problem. Therefore, from (11) we can write

$$\frac{1}{t_1} \int_0^{t_1} \{f(\theta) - Z(\theta)\,\mathrm{sign}[\lambda_1 Z(\theta) + \lambda_2]\,\bar{u}\}\, dt > \frac{1}{t_1} \int_0^{t_1} f(\theta)\, dt \geq 0$$

for the minimization problem, and

$$0 \leq \frac{1}{t_1} \int_0^{t_1} \{f(\theta) + Z(\theta)\mathrm{sign}[\lambda_1 Z(\theta) + \lambda_2]\,\bar{u}\}\, dt < \frac{1}{t_1} \int_0^{t_1} f(\theta)\, dt$$

for the maximization problem. In the limit as $\bar{u} \to 0$, i.e., external stimulus vanishes, $t_1 \to T$ and the strict inequalities become equalities. For $\bar{u} \neq 0$, these equations yield

$$\int_0^{t_1} Z(\theta)\mathrm{sign}[\lambda_1 Z(\theta) + \lambda_2]dt \leq 0. \tag{13}$$

When the charge-balance constraint is imposed, we require that

$$\int_0^{t_1} u(t)\, dt = \mp\bar{u} \int_0^{t_1} \mathrm{sign}[\lambda_1 Z(\theta) + \lambda_2]dt = 0,$$

which yields

$$\int_0^{t_1} \mathrm{sign}[\lambda_1 Z(\theta) + \lambda_2]dt = 0 \tag{14}$$

Also, Eqs. (3) and (10) in this case yield

$$\lambda_1(t_1) = -\frac{1 + \lambda_2 u(t_1)}{f(2\pi) + Z(2\pi)u(t_1)}. \tag{15}$$

When the charge-balance constraint is not imposed, λ_2 and q are eliminated from the system equations. Then (13) becomes

$$\int_0^{t_1} Z(\theta)\mathrm{sign}[\lambda_1 Z(\theta)]\, dt \leq 0. \tag{16}$$

We note that, from (5), $\lambda_1 = 0$ defines an invariant surface, so if $\lambda_1(0) < 0$ then λ_1 will remain negative, or if $\lambda_1(0) > 0$ then λ_1 will remain positive, i.e., λ_1 is a uni-sign function. Therefore, in (16), $\mathrm{sign}[\lambda_1 Z(\theta)]$ is either $+\mathrm{sign}[Z(\theta)]$ or $-\mathrm{sign}[Z(\theta)]$, where the plus and the minus signs represent the sign of $\lambda_1(t)$. In order to have (16) satisfied, necessarily, we must have $\lambda_1(t) < 0$ for all t. This simplifies (8) and (9) to

$$u^*(t) = \pm\mathrm{sign}\left[Z[\theta^*(t)]\right]\bar{u}, \tag{17}$$

for the case where charge-balance is not considered. This is in accordance with the argument made in Moehlis et al. (2006) which shows that the time-optimal control (17) extremizes the right hand side of (1) and so is a sufficient condition for achieving the extremum of ISI.

3 Examples

We now solve this time optimal control problem for examples of Type I and Type II neurons (Hansel et al. 1995). Type I neurons are those that have a non-negative PRC for all phases, i.e., $Z(\theta) \geq 0$ for all θ. For these neurons, any positive (resp., negative)

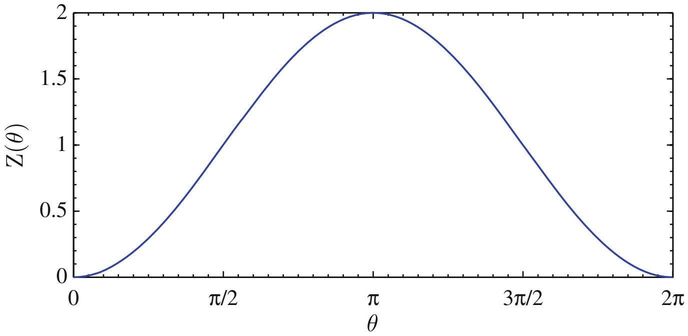

Fig. 1 SNIPER PRC with $Z_d = 1$

impulsive input stimulus will advance (resp., retard) the phase regardless of the time at which the stimulus is applied. For Type II neurons, on the other hand, the PRC takes both positive and negative values. Therefore, an impulsive input stimulus could advance or retard the phase depending on the time at which it is applied. The PRC for a neuron can be obtained experimentally, numerically, or in some cases, analytically.

Specifically, we consider four different neuron models: the SNIPER model, theta neuron model, sinusoidal model, and phase-reduced Hodgkin–Huxley model. The SNIPER model arises when the periodic orbit corresponding to periodic firing of the neuron comes from a Saddle-Node bifurcation of two fixed points on an Infinite PERiod orbit (SNIPER bifurcation). Close to the bifurcation point one can analytically approximate the associated PRC; since this turns out to be non-negative, it is a Type I PRC (Ermentrout 1996; Brown et al. 2004b). The theta neuron model generalizes the SNIPER model to include the non-oscillatory regime (Ermentrout 1996). On the other hand, if the bifurcation which gives the periodic orbit corresponding to periodic firing of the neuron is a saddle-node bifurcation of periodic orbits, then one can approximate the PRC as sinusoidal, giving the sinusoidal model (Brown et al. 2004b); this corresponds to a Type II PRC. Finally, the phase-reduced Hodgkin–Huxley model uses the PRC for the Hodgkin–Huxley equations calculated numerically using XPPAUT, which solves the appropriate adjoint equations (Ermentrout 2002; Brown et al. 2004b).

3.1 SNIPER model

In this model, $Z(\theta) = Z_d(1 - \cos(\theta))$ (see Fig. 1) and $f(\theta) = \omega =$ constant, where $Z_d > 0$ is a constant (Ermentrout 1996; Brown et al. 2004b). Equations (11) and (12) become

$$\dot{\theta} = \omega \mp Z_d(1 - \cos(\theta))\text{sign}[\lambda_1 Z_d(1 - \cos(\theta)) + \lambda_2]\bar{u}, \tag{18}$$

$$\dot{\lambda}_1 = \pm\lambda_1 Z_d \sin(\theta)\text{sign}[\lambda_1 Z_d(1 - \cos(\theta)) + \lambda_2]\bar{u}, \tag{19}$$

where, as before, the signs on top are for the minimization problem, and those on the bottom are for the maximization problem. We consider two cases, namely, with the charge-balance constraint and without it.

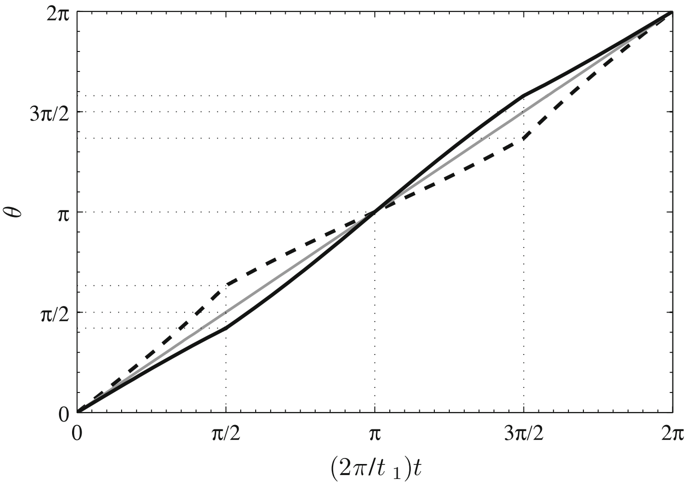

Fig. 2 Evolution of θ in time for $\bar{u} \equiv 0$ (*solid gray line*) corresponding to the neuron's intrinsic firing and $\bar{u} = 0.2$ for both the minimization (*solid black line*) and the maximization (*dashed line*) problems. We see that at $t = \frac{t_1}{4}$, marked as $\pi/2$ on the scaled horizontal axis, when $\bar{u} \equiv 0$, $\theta(\frac{t_1}{4}) = \frac{\pi}{2}$, when $\bar{u} \neq 0$, for the minimization problem $\theta(\frac{t_1}{4}) < \frac{\pi}{2}$ and for the maximization problem $\theta(\frac{t_1}{4}) > \frac{\pi}{2}$

With charge-balance constraint: When the charge-balance constraint (14) is imposed, Eq. (13) becomes

$$\int_0^{t_1} \cos(\theta)\mathrm{sign}[\lambda_1 Z_d(1 - \cos(\theta)) + \lambda_2]\, dt > 0. \tag{20}$$

The solution that satisfies (20) and maximizes (resp., minimizes) the average angular velocity in the righthand side of (18) subject to (14), is one that the function sign[·] varies according to the following:

$$\begin{array}{ll} \mathrm{sign}[\lambda_1(1 - \cos(\theta)) + \lambda_2] = -1, & \frac{t_1}{4} \le t \le \frac{3t_1}{4}, \\ \mathrm{sign}[\lambda_1(1 - \cos(\theta)) + \lambda_2] = \;\;\, 1, & \text{otherwise.} \end{array} \tag{21}$$

To see this, we point out that maximizing (resp., minimizing) the average angular velocity in (18) amounts to minimizing the function $\int_0^{t_1}(1 - \cos(\theta))\mathrm{sign}[\cdot]dt$. Considering the graph of $(1 - \cos(\theta))$ in Fig. 1, it is readily inferred that the value of this integral is most effectively reduced if the sign[·] function is -1 when $(1 - \cos(\theta))$ has largest area under curve, that is for intermediate values of θ. Since we also require (14), the sign[·] function has to change as indicated in (21) to achieve most effective minimization. Note that in the presence of external stimuli, even though $\theta(0) = 0$ and $\theta(t_1) = 2\pi$, but $\theta(\frac{t_1}{4}) \neq \frac{\pi}{2}$ and $\theta(\frac{3t_1}{4}) \neq \frac{3\pi}{2}$ as shown in Fig. 2. Equations (21) yield

$$\begin{array}{ll} u^*(t) = \pm\bar{u}, & \frac{t_1}{4} \le t \le \frac{3t_1}{4}, \\ u^*(t) = \mp\bar{u}, & \text{otherwise.} \end{array} \tag{22}$$

From (21), (18) and (19) become

$$\begin{aligned} \dot{\theta} &= \omega \pm Z_d(1-\cos(\theta))\bar{u}, && \tfrac{t_1}{4} \le t \le \tfrac{3t_1}{4}, \\ \dot{\theta} &= \omega \mp Z_d(1-\cos(\theta))\bar{u}, && \text{otherwise}, \end{aligned} \tag{23}$$

$$\begin{aligned} \dot{\lambda}_1 &= \mp\lambda_1 Z_d \sin(\theta)\bar{u} && \tfrac{t_1}{4} \le t \le \tfrac{3t_1}{4}, \\ \dot{\lambda}_1 &= \pm\lambda_1 Z_d \sin(\theta)\bar{u} && \text{otherwise}. \end{aligned} \tag{24}$$

These equations are symmetric about $t = \frac{t_1}{2}$, meaning that the (θ, λ_1) trajectories take on identical values for $t = \frac{t_1}{2} - \delta$ and $t = \frac{t_1}{2} + \delta$ for all $\delta \in [0, \frac{t_1}{2}]$, which implies $\theta(\frac{t_1}{2}) = \pi$ and $\lambda_1(0) = \lambda_1(t_1)$. Since $\lambda_1 = 0$ is an invariant set, λ_1 is either always positive or always negative. In order to determine the sign of λ_1 we note that we want to satisfy (21). Considering the shape of the PRC function in Fig. 1, one can verify that the only way to arrive at (21) is to have a negative $\lambda_1(t)$ to flip and scale $(1-\cos(\theta))$ function and a positive scalar value λ_2 to shift the product $\lambda_1(1-\cos(\theta))$ up along the vertical axis just enough for (21) to be satisfied. This amounts to having $\lambda_1(0) < 0$ with $\lambda_2 = -\lambda_1(\frac{t_1}{4})Z_d(1-\cos(\theta_a)) > 0$, where $\theta_a = \theta(\frac{t_1}{4})$, for both the minimization and maximization problems.

From (15), we get

$$\lambda_1(0) = -\frac{1}{\omega}(1 \mp \lambda_2 \bar{u}), \tag{25}$$

where we have used the facts that $Z(2\pi) = 0$ and $\lambda_1(0) = \lambda_1(t_1)$. In order to have $\lambda_1(0) < 0$, from (25), we conclude that we must have $\lambda_2 < \frac{1}{\bar{u}}$, which gives an upper bound for λ_2 for the minimization problem.

By symmetry, $\theta(\frac{t_1}{2}) = \pi$. Thus, from (23), provided $\dot{\theta} > 0$ for all times,

$$\int_0^{t_1/2} dt = \int_0^{\theta_a} \frac{d\theta}{\omega \mp Z_d(1-\cos(\theta))\bar{u}} + \int_{\theta_a}^{\pi} \frac{d\theta}{\omega \pm Z_d(1-\cos(\theta))\bar{u}}, \tag{26}$$

where $\theta_a = \theta(\frac{t_1}{4})$. In order to solve Eq. (26) in terms of t_1, first θ_a needs to be determined. We realize that by construction, the first integral in (26) is valid for $t \in [0, \frac{t_1}{4})$ and the second integral is valid for $t \in [\frac{t_1}{4}, \frac{t_1}{2}]$. So solving the first integral in (26), setting the result equal to $\frac{t_1}{4}$ in the limit, and solving for θ_a, one gets

$$\begin{aligned} \theta_a &= 2\arctan\left[\sqrt{\tfrac{\omega}{\omega - 2Z_d\bar{u}}}\ \tan\left(\tfrac{t_1}{8}\sqrt{\omega(\omega - 2Z_d\bar{u})}\right)\right], && 0 \le \bar{u} < \tfrac{\omega}{2Z_d} \\ \theta_a &= 2\arctan\left[\tfrac{t_1}{8}\omega\right], && \bar{u} = \tfrac{\omega}{2Z_d} \\ \theta_a &= 2\arctan\left[\sqrt{\tfrac{\omega}{2Z_d\bar{u} - \omega}}\ \tanh\left(\tfrac{t_1}{8}\sqrt{\omega(2Z_d\bar{u} - \omega)}\right)\right], && \bar{u} > \tfrac{\omega}{2Z_d} \end{aligned}$$

for the minimization problem and

$$\theta_a = 2\arctan\left[\sqrt{\tfrac{\omega}{2Z_d\bar{u}+\omega}}\ \tan\left(\tfrac{t_1}{8}\sqrt{\omega(2Z_d\bar{u}+\omega)}\right)\right], \qquad 0 \le \bar{u} < \tfrac{\omega}{2Z_d}$$

for the maximization problem. In both of these cases, when $\bar{u} \equiv 0$, $t_1 = T = \frac{2\pi}{\omega}$ and $\theta_a = \frac{\pi}{2}$. However, when $\bar{u} \neq 0$, $0 < \theta_a < \frac{\pi}{2}$ for the minimization problem and $\frac{\pi}{2} < \theta_a < \pi$ for the maximization problem. Figure 2 shows the evolution of θ in time for when $\bar{u} \equiv 0$ (intrinsic firing) and for when $\bar{u} = 0.2$ for both the minimization and the maximization problems. Note that the time axis in scaled so that 0, $\frac{\pi}{2}$, π, $\frac{3\pi}{2}$, and 2π points on the horizontal axis correspond to $t = 0$, $\frac{t_1}{4}$, $\frac{t_1}{2}$, $\frac{3t_1}{4}$, and t_1, respectively.

Now solving the second integral in (26) with these θ_a values results in the following implicit expressions for t_1:

$$\begin{array}{ll}
\frac{t_1}{8}\sqrt{\omega(2Z_d\bar{u}+\omega)} = \frac{\pi}{2} - \arctan\left[\sqrt{\frac{2Z_d\bar{u}+\omega}{\omega-2Z_d\bar{u}}}\tan\left(\frac{t_1}{8}\sqrt{\omega(\omega-2Z_d\bar{u})}\right)\right], & 0 \le \bar{u} < \frac{\omega}{2Z_d} \\
\frac{\sqrt{2}}{8}t_1\omega = \frac{\pi}{2} - \arctan\left[\frac{\sqrt{2}}{8}t_1\omega\right], & \bar{u} = \frac{\omega}{2Z_d} \\
\frac{t_1}{8}\sqrt{\omega(2Z_d\bar{u}+\omega)} = \frac{\pi}{2} - \arctan\left[\sqrt{\frac{2Z_d\bar{u}+\omega}{2Z_d\bar{u}-\omega}}\tanh\left(\frac{t_1}{8}\sqrt{\omega(2Z_d\bar{u}-\omega)}\right)\right], & \bar{u} > \frac{\omega}{2Z_d}
\end{array} \tag{27}$$

for the minimization problem and

$$\frac{t_1}{8}\sqrt{\omega(\omega-2Z_d\bar{u})} = \frac{\pi}{2} - \arctan\left[\sqrt{\frac{\omega-2Z_d\bar{u}}{\omega+2Z_d\bar{u}}}\tan\left(\frac{t_1}{8}\sqrt{\omega(\omega+2Z_d\bar{u})}\right)\right], \quad 0 \le \bar{u} < \frac{\omega}{2Z_d} \tag{28}$$

for the maximization problem.

In order to find an explicit formula for t_1, we Taylor expand (27) and (28) for small $\bar{u}$ and solve for t_1 to obtain

$$t_1 = \frac{2\pi}{\omega} \mp \frac{4Z_d}{\omega^2}\bar{u} + \frac{\pi Z_d^2}{\omega^3}\bar{u}^2 + \mathcal{O}(\bar{u}^3), \tag{29}$$

where the top sign is for the minimization problem and the bottom sign for the maximization problem.

It is worth pointing out that in writing (26), we have assumed that $\dot{\theta} > 0$ for all times. Considering (23), we see that for the minimization problem, $\dot{\theta} > 0$ implies that when $t \notin [\frac{t_1}{4}, \frac{3t_1}{4}]$, we must have $\bar{u} < \frac{\omega}{Z_d(1-\cos(\theta_a))}$ for all $\bar{u}$. Lemma 2 proves that regardless of $\bar{u}$ this statement, which is equivalent to saying $\dot{\theta} > 0$, is always true, although we recall that the phase model is only valid for sufficiently small $\bar{u}$. For the maximization problem, when $t \notin [\frac{t_1}{4}, \frac{3t_1}{4}]$, $\dot{\theta}$ is positive, but when $t \in [\frac{t_1}{4}, \frac{3t_1}{4}]$, $\dot{\theta}$ would be positive provided $\bar{u} < \frac{\omega}{Z_d(1-\cos(\pi))} = \frac{\omega}{2Z_d}$.

Lemma 2 *Consider* (23). *For the minimization problem, we have*

$$\dot{\theta} > 0 \quad \forall \bar{u} \quad \text{for } 0 \le t \le \frac{t_1}{4} \quad \text{and} \quad \frac{3t_1}{4} \le t \le t_1. \tag{30}$$

Proof First consider $0 \le t \le \frac{t_1}{4}$. We consider three cases: $\bar{u} < \frac{\omega}{Z_d}$, $\bar{u} = \frac{\omega}{Z_d}$, and $\bar{u} > \frac{\omega}{Z_d}$. If $\bar{u} < \frac{\omega}{Z_d}$, then $\min \dot{\theta} = \dot{\theta}(\frac{t_1}{4}) = \omega - Z_d(1 - \cos(\theta_a))\bar{u} > \omega - Z_d\bar{u} > 0$ since $0 < \theta_a < \pi/2$. The last inequality follows from the fact that the input over this time interval slows down the phase evolution of the neuron, so it does not reach a quarter of its total desired phase change of 2π in a quarter of the total time t_1. If $\bar{u} = \frac{\omega}{Z_d}$, then $\min \dot{\theta} = \dot{\theta}(\frac{t_1}{4}) = \omega \cos(\theta_a) > 0$ as $\theta_a < \frac{\pi}{2}$ for the minimization problem. If $\bar{u} > \frac{\omega}{Z_d}$, then let $\bar{\theta} = \min(\arccos(1 - \frac{\omega}{Z_d\bar{u}}), \theta_a)$, where $\arccos(1 - \frac{\omega}{Z_d\bar{u}})$ is where $\dot{\theta}$ becomes zero first and θ_a is where the control switches (before $\dot{\theta}$ becomes negative). This way, we can say that for $0 < \theta \le \bar{\theta}$, we have $\dot{\theta} \ge 0$ and $\min \dot{\theta} = \omega - Z_d(1 - \cos(\bar{\theta}))\bar{u}$. We can write

$$\int_0^{\bar{t}} dt = \int_0^{\bar{\theta}} \frac{d\theta}{\omega - Z_d(1 - \cos(\theta))\bar{u}},$$

which yields

$$\bar{t} = \frac{2}{\sqrt{\omega(2Z_d\bar{u} - \omega)}} \operatorname{arctanh}\left[\sqrt{\frac{2Z_d\bar{u} - \omega}{\omega}} \tan\left(\frac{\bar{\theta}}{2}\right)\right], \tag{31}$$

where $\bar{t}$ is the time at which $\theta = \bar{\theta}$. Now if $\bar{\theta} = \theta_a$, meaning $\bar{t} = \frac{t_1}{4} < +\infty$ then we must have $0 < \sqrt{\frac{2Z_d\bar{u} - \omega}{\omega}} \tan(\frac{\theta_a}{2}) < 1$ for the $\operatorname{arctanh}(\cdot)$ function to be real, which from (47) implies $\dot{\theta}(\frac{t_1}{4}) = \omega - Z_d(1 - \cos(\theta_a))\bar{u} > 0$.

However, if $\bar{\theta} \to \arccos(1 - \frac{\omega}{Z_d\bar{u}})$ then it is inferred that $\bar{t} < \frac{t_1}{4} < +\infty$. From (31) we see that as $\bar{\theta} \to \arccos(1 - \frac{\omega}{Z_d\bar{u}})$, $\bar{t} \to +\infty$ which contradicts $\bar{t} < \frac{t_1}{4} < +\infty$. So t always reaches $\frac{t_1}{4}$ before $\dot{\theta}$ becomes negative. We remark that by symmetry, these results also imply that $\dot{\theta} > 0$ for $\frac{3t_1}{4} \le t \le t_1$. □

Without charge-balance constraint: When the charge-balance constraint is not imposed the optimal current is given by (17). For the SNIPER PRC, this optimal current further simplifies to

$$u^*(t) = \pm\bar{u}, \tag{32}$$

resulting in

$$\dot{\theta} = \omega \pm Z_d(1 - \cos(\theta))\bar{u}. \tag{33}$$

Since the PRC is symmetric about $\theta = \pi$, one can integrate this equation and write

$$\int_0^{t_1/2} dt = \int_0^{\pi} \frac{d\theta}{\omega \pm Z_d(1 - \cos(\theta))\bar{u}},$$

which yields

$$t_1 = \frac{2\pi}{\sqrt{\omega(\omega \pm 2Z_d\bar{u})}}. \tag{34}$$

It should be noted that in order to make sure $\dot{\theta}$ in (33) is always positive, for the maximization problem, we must have $\bar{u} < \frac{\omega}{2Z_d}$.

Figure 3a shows the extreme values for the ISI (or t_1) as a function of $\bar{u}$ for this model. As can be seen in this figure, applying the charge-balance constraint has a notable effect on the value of the extreme t_1. This is due to the fact that the optimal control inputs that we achieve with this model without imposing the charge-balance constraint are always either positive or negative, and thus very different from the charge-balanced control inputs.

3.2 Theta neuron model

In this model, $Z(\theta) = 1 - \cos(\theta)$ and $f(\theta) = 1 + \cos(\theta) + I_b(1 - \cos(\theta))$. In the absence of control input, the dynamics of this neuron model are such that for $I_b > 0$ the neuron fires periodically with a natural angular velocity of $\omega = 2\sqrt{I_b}$. However, when $I_b < 0$, the neuron is said to be excitable, i.e., upon injection of some appropriate input stimuli it would start to fire periodically; otherwise it would not fire at all (Ermentrout 1996; Moehlis et al. 2006).

In order to investigate the effect of a control input on the firing time of the neuron, we again consider two cases, namely, a control input with charge-balance constraint and one without it.

With charge-balance constraint: Since this model has the same PRC as the SNIPER model (with $Z_d = 1$), similar arguments can be used to arrive at (21) and (22), giving

$$\begin{aligned} \dot{\theta} &= (1 + I_b \pm \bar{u}) + \cos(\theta)\,(1 - (I_b \pm \bar{u}))\,, && \tfrac{t_1}{4} \le t \le \tfrac{3t_1}{4}, \\ \dot{\theta} &= (1 + I_b \mp \bar{u}) + \cos(\theta)\,(1 - (I_b \mp \bar{u}))\,, && \text{otherwise}, \end{aligned} \tag{35}$$

$$\begin{aligned} \dot{\lambda}_1 &= -\lambda_1 \sin(\theta)(I_b \pm \bar{u} - 1), && \tfrac{t_1}{4} \le t \le \tfrac{3t_1}{4}, \\ \dot{\lambda}_1 &= -\lambda_1 \sin(\theta)(I_b \mp \bar{u} - 1), && \text{otherwise}. \end{aligned} \tag{36}$$

As in the case of SNIPER model, due to the symmetry that these equations have about $t = \frac{t_1}{2}$, we have $\theta(\frac{t_1}{2}) = \pi$ and $\lambda_1(0) = \lambda_1(t_1)$. Also λ_1 is either always negative or always positive. By considering the shape of the PRC, one can easily verify that we need $\lambda_1(0) < 0$ together with $\lambda_2 = -\lambda_1(\frac{t_1}{4})(1 - \cos(\theta_a)) > 0$, where $\theta_a = \theta(\frac{t_1}{4})$, in order to satisfy (21) for both the minimization and maximization problems.

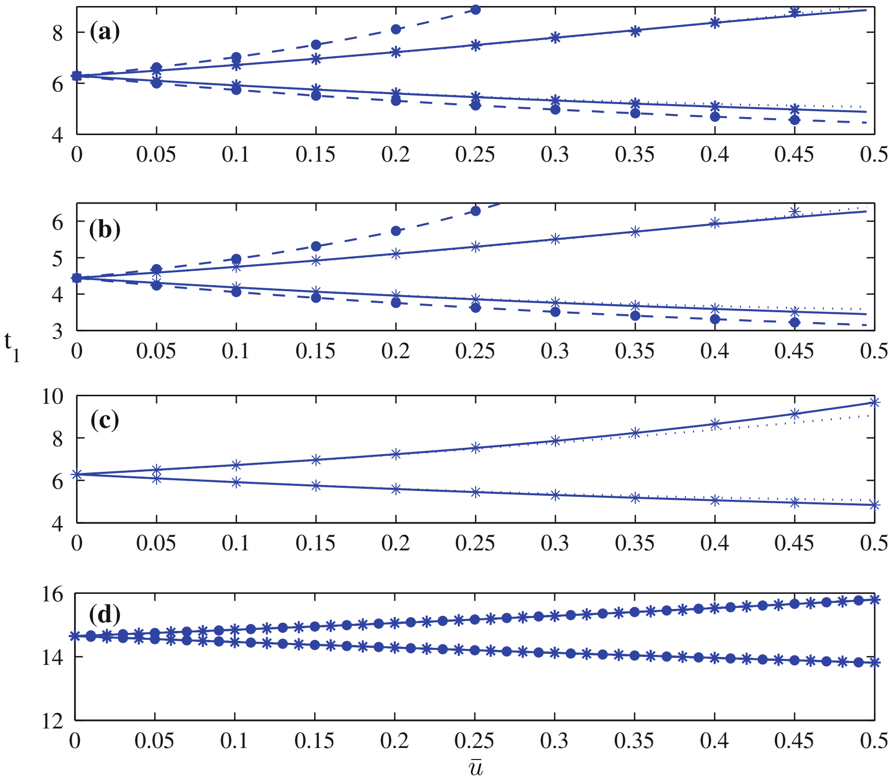

Fig. 3 Extreme ISI (or t_1) values as functions of the control bound $\bar{u}$. **a–c** Results for the SNIPER, theta neuron, and sinusoidal models, respectively. For these results, $\omega = 1$ rad/s, $Z_d = 1$, and $I_b = 0.5$ have been chosen where applicable. The *solid lines* are the extreme t_1 for the charge-balanced optimal control case for the maximization (*top solid line*) and minimization (*bottom solid line*) problems obtained from the analytical formulas provided in the text. The *dashed lines* are the results without the charge-balance constraint. (For the sinusoidal model, since the results with or without the charge-balance constraint are identical, the *dashed lines* have not been shown.) The *dotted lines* are the second order approximations for t_1 while the star and circle markers are the results obtained from numerical simulation for the cases with and without the charge-balance constraint, respectively. **d** Numerical results for the phase-reduced Hodgkin–Huxley model with standard parameters given in Appendix, where again the *solid lines* and the *star* markers are for the case with the charge-balance constraint and the *dashed lines* and the *circle marks* are for the case without the constraint. We see that the constraint has negligible effect on the results for this model

Furthermore, we want to make sure that $\dot{\theta} > 0$ for all $0 < t < t_1$. Considering (35), for the minimization problem, when $t \in [\frac{t_1}{4}, \frac{3t_1}{4}]$, $\dot{\theta}$ would be positive provided $(I_b + \bar{u}) > -\frac{1+\cos(\pi)}{1-\cos(\pi)} = 0$. For $t \notin [\frac{t_1}{4}, \frac{3t_1}{4}]$, we need $(I_b - \bar{u}) > -\frac{1+\cos(\theta_a)}{1-\cos(\theta_a)}$ in order to guarantee a positive $\dot{\theta}$. Lemma 3 proves that for arbitrary $(I_b - \bar{u})$ this criterion is always satisfied. In summary, for the minimization problem, taking $I_b + \bar{u} > 0$ will guarantee that $\dot{\theta} > 0$ for all times.

Similarly, for the maximization problem, one arrives at the requirement that $I_b - \bar{u} > 0$ (which means $I_b + \bar{u} > 0$ since $\bar{u} > 0$) for a positive $\dot{\theta}$.

Lemma 3 *For the minimization problem of the theta neuron model, when* $0 \leq t \leq \frac{t_1}{4}$, *for arbitrary* $I_b - \bar{u}$ *we have*

$$\dot{\theta} = (1 + I_b - \bar{u}) + \cos(\theta)(1 - (I_b - \bar{u})) > 0 \quad \forall \bar{u} \geq 0. \tag{37}$$

Proof For $I_b - \bar{u} > 0$, this is trivial, because one can easily rearrange (37) and write $\dot{\theta} = 1 + \cos(\theta) + (I_b - \bar{u})(1 - \cos(\theta))$, which is exactly the equation for a non-stimulated theta neuron model with $(I_b - \bar{u})$ substituted for I_b.

For $I_b - \bar{u} \leq 0$, when $\theta = 0$ we have $\dot{\theta} = 2 > 0$. So, for $\dot{\theta}$ to become negative, it has to become zero first. Assume at $t = \bar{t} < +\infty$, $\theta(\bar{t}) = \bar{\theta} = \arccos(\frac{I_b - \bar{u} + 1}{I_b - \bar{u} - 1})$ for which $\dot{\theta}$ vanishes. Integrating the system in (37), we obtain

$$\bar{t} = \frac{1}{\sqrt{\bar{u} - I_b}} \operatorname{arctanh}\left[\sqrt{\bar{u} - I_b} \tan\left(\frac{\bar{\theta}}{2}\right)\right]. \tag{38}$$

Now if $\theta(\bar{t}) \to \arccos(\frac{I_b - \bar{u} + 1}{I_b - \bar{u} - 1})$ then, using the identity $\cos(\theta) = 2\cos^2(\frac{\theta}{2}) - 1$, one can easily verify that $\tan(\frac{\bar{\theta}}{2}) \to \sqrt{\frac{1}{\bar{u} - I_b}}$, implying $\bar{t} \to +\infty$, which in turn contradicts the assumption of $\bar{t}$ being finite. Thus, $\dot{\theta} > 0$ for $0 \leq t \leq \frac{t_1}{4}$ and $\theta_a < \bar{\theta}$ regardless of how negative $(I_b - \bar{u})$ is. □

In order to obtain an analytical solution for t_1, one can perform similar calculations as for the SNIPER model case by writing

$$\int_0^{t_1/2} dt = \int_0^{\theta_a} \frac{d\theta}{(1 + I_b \pm \bar{u}) + \cos(\theta)\,(1 - (I_b \pm \bar{u}))} + \int_{\theta_a}^{\pi} \frac{d\theta}{(1 + I_b \mp \bar{u}) + \cos(\theta)\,(1 - (I_b \mp \bar{u}))},$$

where $\theta_a = \theta(\frac{t_1}{4})$, giving the following implicit formulas for t_1:

$$\begin{aligned} &\tfrac{t_1}{4}\sqrt{I_b + \bar{u}} = \tfrac{\pi}{2} - \arctan\left[\sqrt{\tfrac{I_b + \bar{u}}{I_b - \bar{u}}} \tan\left(\tfrac{t_1}{4}\sqrt{I_b - \bar{u}}\right)\right], && I_b - \bar{u} > 0 \\ &\tfrac{t_1}{4}\sqrt{2I_b} = \tfrac{\pi}{2} - \arctan\left[\tfrac{t_1}{4}\sqrt{2I_b}\right], && I_b = \bar{u} \\ &\tfrac{t_1}{4}\sqrt{I_b + \bar{u}} = \tfrac{\pi}{2} - \arctan\left[\sqrt{\tfrac{\bar{u} + I_b}{\bar{u} - I_b}} \tanh\left(\tfrac{t_1}{4}\sqrt{\bar{u} - I_b}\right)\right], && I_b - \bar{u} < 0 \end{aligned} \tag{39}$$

for the minimization problem, where $I_b + \bar{u} > 0$, and

$$\tfrac{t_1}{4}\sqrt{I_b - \bar{u}} = \tfrac{\pi}{2} - \arctan\left[\sqrt{\tfrac{I_b - \bar{u}}{I_b + \bar{u}}} \tan\left(\tfrac{t_1}{4}\sqrt{I_b + \bar{u}}\right)\right], \quad I_b - \bar{u} > 0 \tag{40}$$

for the maximization problem.

In order to find an explicit formula for t_1, we Taylor expand the first equation in (39) and (40) for small $\bar{u}$ and solve for t_1 to obtain

$$t_1 = \frac{\pi}{\sqrt{I_b}} \mp I_b^{-\frac{3}{2}}\bar{u} + \frac{\pi}{8} I_b^{-\frac{5}{2}}\bar{u}^2 + \mathcal{O}(\bar{u}^3), \tag{41}$$

where the top sign is for the minimization problem and the bottom sign for the maximization problem. We note that, for the minimization problem, for $I_b - \bar{u} \le 0$, we do not have an approximation for t_1. We cannot use the second and third equations in (39) for small $\bar{u}$ as they lead to $I_b + \bar{u} \le 0$ in the limit $\bar{u} \to 0$, violating the validity domain for (39).

Without charge-balance constraint: Since the theta neuron model has a PRC with the same shape as for the SNIPER model, when the charge-balance constraint is not imposed the optimal control input would be the same as (32), resulting in:

$$\frac{t_1}{2} = \int_0^{\pi} \frac{d\theta}{1 + \cos(\theta) + (1 - \cos(\theta))(I_b \pm \bar{u})}.$$

This yields

$$t_1 = \frac{\pi}{\sqrt{I_b \pm \bar{u}}}, \quad I_b \pm \bar{u} > 0. \tag{42}$$

We point out that when the charge-balance constraint is not imposed, we need to have $I_b + \bar{u} > 0$ for the minimization problem, and $I_b - \bar{u} > 0$ for the maximization problem in order to have oscillatory motion; this is analogous to the requirement for I_b in the absence of a control input.

Figure 3b shows the extreme values for ISI (or t_1) as a function of $\bar{u}$ for this model. We see that applying the charge-balance constraint has a notable effect on the value of the extreme t_1. This is due to the fact that the optimal control inputs that we achieve with this model when the charge-balance constraint is not imposed are, similar to the SNIPER model case, always either positive or negative and thus very different from the charge-balanced control inputs.

3.3 Sinusoidal model

In this model, $Z(\theta) = Z_d \sin(\theta)$ and $f(\theta) = \omega =$ constant, where $Z_d > 0$ is a constant. The PRC for this model is perfectly symmetric with respect to the point $\theta = \pi$. If one attempts to solve the time optimization problem without considering the charge-balance constraint, one would use (17) for the optimal control input. This yields

$$\begin{aligned} \dot{\theta} &= \omega \pm Z_d \sin(\theta)\bar{u}, \quad 0 \le \theta < \pi, \\ \dot{\theta} &= \omega \mp Z_d \sin(\theta)\bar{u}, \quad \pi \le \theta < 2\pi. \end{aligned} \tag{43}$$

In addition, considering the symmetry of the PRC about $\theta = \pi$, it follows that if the system is to evolve from $\theta(0) = 0$ to $\theta(t_1) = 2\pi$, then it would satisfy $\theta(\frac{t_1}{2}) = \pi$. This means that the optimal current in (17) changes sign at $t = \frac{t_1}{2}$, which implies that it is actually charge-balanced. If one solves the Euler-Lagrange equations in (4)–(8)/(9), one would get $\lambda_2 \equiv 0$ for this model, which implies that the optimal control inputs are always charge-balanced regardless of imposing the charge-balance constraint or not.

In this model, when $0 \leq \theta \leq \pi$, $\dot{\theta}$ takes on identical values with respect to $\theta = \frac{\pi}{2}$, i.e., $\dot{\theta}(\frac{\pi}{2} - \delta) = \dot{\theta}(\frac{\pi}{2} + \delta)$ for $\delta \in [0, \frac{\pi}{2}]$. This means that θ evolves from 0 to $\frac{\pi}{2}$ in exactly the same time as it evolves from $\frac{\pi}{2}$ to π, which implies that $\theta(t = \frac{t_1}{4}) = \frac{\pi}{2}$. Also, we want to make sure that $\dot{\theta} > 0$ for all times. This is always the case for the minimization problem, but for the maximization problem it will only hold if $\bar{u} < \frac{\omega}{Z_d}$.

One can now calculate the optimal spiking time by integrating (43):

$$\int_0^{t_1/4} dt = \int_0^{\pi/2} \frac{d\theta}{\omega \pm Z_d \sin(\theta)\bar{u}}.$$

This yields

$$\begin{aligned}
t_1 &= \frac{8}{\sqrt{\omega^2 - Z_d^2\bar{u}^2}} \arctan\left[\sqrt{\frac{\omega - Z_d\bar{u}}{\omega + Z_d\bar{u}}}\right], && 0 \leq \bar{u} < \tfrac{\omega}{Z_d} \\
t_1 &= \frac{4}{\omega}, && \bar{u} = \tfrac{\omega}{Z_d} \\
t_1 &= \frac{8}{\sqrt{Z_d^2\bar{u}^2 - \omega^2}} \operatorname{arctanh}\left[\sqrt{\frac{Z_d\bar{u} - \omega}{Z_d\bar{u} + \omega}}\right], && \bar{u} > \tfrac{\omega}{Z_d}
\end{aligned} \tag{44}$$

for the minimization problem, and

$$t_1 = \frac{8}{\sqrt{\omega^2 - Z_d^2\bar{u}^2}} \arctan\left[\sqrt{\frac{\omega + Z_d\bar{u}}{\omega - Z_d\bar{u}}}\right], \quad 0 \leq \bar{u} < \tfrac{\omega}{Z_d} \tag{45}$$

for the maximization problem.

In order to find an approximation to t_1, we Taylor expand (44) and (45) for small $\bar{u}$ and solve for t_1 to obtain

$$t_1 = \frac{2\pi}{\omega} \mp \frac{4Z_d}{\omega^2}\bar{u} + \frac{\pi Z_d^2}{\omega^3}\bar{u}^2 + \mathcal{O}(\bar{u}^3). \tag{46}$$

Figure 3c shows the extreme values for the ISI (or t_1) as a function of $\bar{u}$ for this model. As mentioned before, applying the charge-balance constraint here has no effect on the value of the extreme t_1. This is due to the fact that the optimal control inputs that

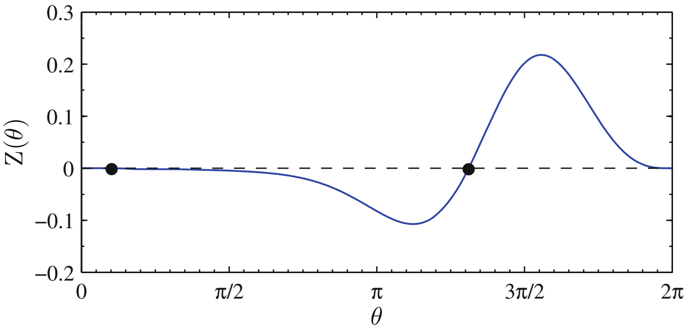

Fig. 4 Hodgkin–Huxley PRC, obtained numerically using XPPAUT with $I_b = 10$. *Dots* indicate where $Z = 0$

we achieve with the sinusoidal model without imposing the charge-balance constraint are exactly charge-balanced themselves.

3.4 Phase-reduced Hodgkin–Huxley model

The Hodgkin–Huxley equations are a conductance-based model for neurons proposed in 1952 as a result of a series of experiments on the giant axon of a squid (Hodgkin and Huxley 1952). This model has become the prototypical model for neuronal membrane dynamics. Although not representing human brain neurons, the Hodgkin–Huxley model exhibits oscillatory behavior, as do human motor control neurons in the thalamus and basal ganglia regions of the brain. The equations and parameters of this model are presented in the Appendix.

The PRC for this model has been calculated numerically using XPPAUT (Ermentrout 2002) with time steps of 0.005 ms, see Fig. 4. The specifics of this PRC are:

$$\begin{aligned} &Z(0) = Z(2\pi) = 7.7 \times 10^{-5}, \\ &Z(0.354) = Z(4.120) = 0, \\ &Z(\theta) < 0 \quad 0.354 < \theta < 4.120, \\ &Z(\theta) > 0 \quad \text{otherwise}. \end{aligned}$$

Due to the complex shape of this PRC, very little can be said analytically. Thus, we present numerical results for the time optimal problem for this neuron model. In this model, for the parameters that we use, $f(\theta) = \omega = 0.429$ rad/ms = constant which results in $T = 14.63$ ms.

With charge-balance constraint: To solve the TPBVP in this case, given a $\bar{u}$, we initially guess arbitrary values for $\lambda_1(0)$ and t_1. We calculate λ_2 from (15) with $u^*(t_1) = \bar{u}$, and we solve the system of ODE's (4)–(7) for $0 \leq t \leq t_1$ using a shooting method. In this shooting method, we solve the system and if $\theta(t_1) < 2\pi$, we increase t_1 by a certain dt and if $\theta(t_1) > 2\pi$ we decrease t_1 by dt until $|\theta(t_1) - 2\pi| < \epsilon_1$ where ϵ_1 is a predefined tolerance. In other words, we keep *shooting* the system with different t_1

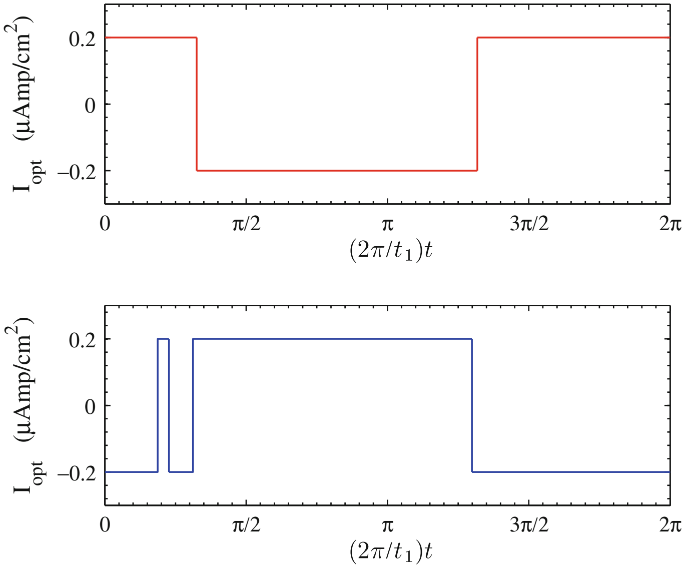

Fig. 5 Optimal control for the Hodgkin–Huxley model with the charge-balance constraint imposed for the minimization problem (*top*) and the maximization problem (*bottom*). The control bound was set $\bar{u} = 0.2$. In the case of the maximization problem, the optimal control has a spike at $(2\pi/t_1)t \approx 0.66$ which is due to a small dent in the PRC for this model at the corresponding location

values until we reach the t_1 that would satisfy this inequality. We note here that in this process, when an upper bound and a lower bound for t_1 is found, the actual value of t_1 is then found by employing the bisection method. Now if $q(t_1) \neq 0$, we conclude that the original guess for $\lambda_1(0)$ had been incorrect. So we perform another shooting process for $\lambda_1(0)$ exactly like the one for t_1, until we find the upper and lower bounds of $\lambda_1(0)$. We then employ the bisection method to converge to the correct $\lambda_1(0)$ for which $|q(t_1)| < \epsilon_2$, where ϵ_2 is a predefined tolerance. Figure 5 shows the results for this model for $\bar{u} = 0.2$. We used fourth order Runge-Kutta for numerical integration.

Without charge-balance constraint: In this case, $\lambda_2 \equiv 0$ and the optimal control is simply given by (17).

Figure 3d shows the extreme values for the ISI (or t_1) as a function of $\bar{u}$ for this model. We see that applying the charge-balance constraint has little effect on the value of the extreme t_1. This is due to the fact that the optimal control inputs that we achieve with the phase-reduced Hodgkin–Huxley model without imposing the charge-balance constraint are *almost* charge-balanced themselves.

In order to see the performance of the phase reduction technique and the phase-reduced Hodgkin–Huxley model, we have solved the phase-reduced model for a number of different $\bar{u}$ values and have obtained the optimal input for each of them. We have then applied these inputs to the full Hodgkin–Huxley equations, given in the Appendix, and have computed the resulting ISI values $t_{1,full}$, to compare with those for the phase-reduced model $t_{1,prm}$. Figure 6 shows the results of this investigation. Recall that the natural period of oscillation for this model is $T = 14.63$ ms. The

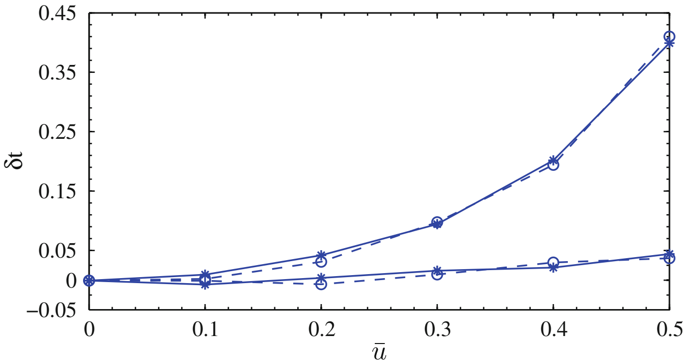

Fig. 6 Comparison between the phase-reduced Hodgkin–Huxley model and the full Hodgkin–Huxley model. $\delta t = t_{1,full} - t_{1,prm}$ is the difference between the t_1 value calculated from the full model and the t_1 value obtained from the phase-reduced model when the $u^*(t)$ obtained from the phase-reduced model is used as the input to both models. The *solid lines* with *asterisk* marks represent the case with the charge-balance constraint and the *dashed lines* with *circle marks* represent the case without the constraint. Also, the *two top lines* are for the maximization problem and the *two bottom lines* are for the minimization problem

phase-reduced model yields accuracy for δt to within one percent for $\bar{u} \leq 0.3$ for the maximization problem and for much larger $\bar{u}$ for the minimization problem.

4 Discussion

We investigated the time optimal control problem for phase models of spiking neurons for which the input is constrained between prespecified upper and lower bounds. The dynamical equations were derived from the Hamiltonian for the system, and the control inputs obtained from Pontryagin's minimum principle, which gives bang-bang control. The problem was considered for two cases: with a charge-balance constraint imposed on the input, and without it. Here the charge-balance constraint ensures that the total electrical charge that is transferred to the neural tissue is zero over the course of one cycle of control input; this is important to prevent neural tissue damage. Analytical expressions for the ISI were derived for these two cases for the SNIPER, theta neuron, and sinusoidal models.

We looked at the SNIPER model as a simplified version of the theta neuron model and as a platform for describing the details of our control strategy. Specifically, we found that in order to have $\dot{\theta} > 0$ at all times, we need not to limit our control input if the minimization problem is considered. However, when considering the maximization problem, $\dot{\theta} > 0$ implies that $\bar{u} < \frac{\omega}{2Z_d}$. The ISI values are then found from (27)–(29) when the charge-balance constraint is imposed and from (34) when the constraint is not imposed.

In the theta neuron model, $I_b \pm \bar{u} > 0$ guarantees $\dot{\theta} > 0$ $\forall t$. The ISI values are then found from (39)–(41) when the charge-balance constraint is imposed and from (42) when the constraint is not imposed.

The sinusoidal model was considered as a simple, yet very insightful, Type II neuron model. It was found that regardless of imposing the charge-balance constraint, the optimal inputs always come out charge balanced. This is due to the symmetry of the

PRC, Eq. (43), as well as the fact that the sinusoidal PRC has equal positive and negative intervals. Due to these specifications, the control input found from the bang-bang optimal control method are always charge balanced. We note that to ensure $\dot{\theta} > 0\ \forall t$, we need to have $\bar{u} < \frac{\omega}{Z_d}$ for the maximization problem, but no such condition on $\bar{u}$ for the minimization problem. This yields (44)–(46) as the ISI values.

We also considered the phase-reduced Hodgkin–Huxley model as a more realistic model for neuronal membrane dynamics and found out that the control input in both cases of with and without the charge-balance constraint are very close to each other. The results from the sinusoidal and Hodgkin–Huxley models suggest that control inputs found for Type II neurons can be almost charge balanced even when the constraint is not imposed.

We also presented numerical results for the phase-reduced Hodgkin–Huxley model as well as for the three other models mentioned. These numerical results agree well with the analytical computations. The performance of the phase reduction method was validated through the close agreement of the ISI values obtained by using the same computed control input for both the phase-reduced and the full Hodgkin–Huxley models.

The results for the ISI presented here are the minimum and maximum values that one can achieve with bounded input stimuli for the aforementioned neuron models on a single neuron level. However, one may consider the problem of finding the $\bar{u}$ that would achieve a prespecified ISI value t_1. We note that depending on the t_1, a $\bar{u}$ may or may not exist. If, for example, we consider a t_1 significantly larger than the neuron's natural period T, then there would not be a $\bar{u}$ that would result in t_1 while satisfying the condition $\dot{\theta} > 0$. As another example, if $t_1 \ll T$, the $\bar{u}$ needed for this would be large and hence outside of the range of validity of phase models as these models are only valid for small inputs. If we choose $t_1 \approx T$, there will be a $\bar{u}$ for the problem, but determining the specific value is not trivial; in particular cases, one can use Eqs. (29), (34), (41), (42), or (46) to find an estimate for or the exact value of the $\bar{u}$.

We note that one can use these results as a foundation for considering the control of a population of neurons. In particular, one can gain insight about the maximum capability of treatment procedures like deep brain stimulation when input stimuli are bounded so as to account for potential practical limitations for the hardware in delivering the input stimulus, as well as the endurance of the biological tissue close to the injection apparatus.

Appendix

Lemma 4 *For the SNIPER model, for* $\omega > 0,\ \bar{u} > \frac{\omega}{Z_d}$, *and* $0 < \theta < \frac{\pi}{2}$,

$$\omega - Z_d(1 - \cos(\theta))\bar{u} > 0 \Leftrightarrow 0 < \tan\left(\frac{\theta}{2}\right) < \sqrt{\frac{\omega}{2Z_d\bar{u} - \omega}}. \tag{47}$$

Proof Given the assumptions of the Lemma, one can write

$$\omega - Z_d(1 - \cos(\theta))\bar{u} > 0 \Leftrightarrow \cos(\theta) > 1 - \frac{\omega}{Z_d\bar{u}} \Leftrightarrow \theta < \arccos\left(1 - \frac{\omega}{Z_d\bar{u}}\right). \tag{48}$$

Let $\alpha = \arccos(1 - \frac{\omega}{Z_d \bar{u}}) < \frac{\pi}{2}$, then

$$\cos^2\left(\frac{\alpha}{2}\right) = \frac{1}{2}\left(1 + \cos(\alpha)\right) = \frac{1}{2}\left(1 + 1 - \frac{\omega}{Z_d \bar{u}}\right) = 1 - \frac{\omega}{2 Z_d \bar{u}},$$
$$\sin^2\left(\frac{\alpha}{2}\right) = 1 - \cos^2\left(\frac{\alpha}{2}\right) = \frac{\omega}{2 Z_d \bar{u}},$$
$$\tan\left(\frac{\alpha}{2}\right) = \sqrt{\frac{\omega}{2 Z_d \bar{u} - \omega}}.$$

Now one can write

$$\begin{aligned} & 0 < \theta < \alpha < \frac{\pi}{2}, \\ \Leftrightarrow \; & 0 < \frac{\theta}{2} < \frac{\alpha}{2} < \frac{\pi}{4}, \\ \Leftrightarrow \; & 0 \leq \tan\left(\frac{\theta}{2}\right) < \tan\left(\frac{\alpha}{2}\right) = \sqrt{\frac{\omega}{2 Z_d \bar{u} - \omega}} < 1, \end{aligned}$$

so, (47) holds. □

Hodgkin–Huxley equations

The full Hodgkin–Huxley model equations are given by:

$$\begin{aligned} \dot{V} &= (I_b + I(t) \overbrace{- \bar{g}_{Na} h (V - V_{Na}) m^3 - \bar{g}_K (V - V_K) n^4 - \bar{g}_L (V - V_L)}^{I_g(V, \mathbf{n})})/c, \\ \dot{m} &= a_m(V)(1 - m) - b_m(V) m, \\ \dot{h} &= a_h(V)(1 - h) - b_h(V) h, \\ \dot{n} &= a_n(V)(1 - n) - b_n(V) n, \end{aligned}$$

$$\begin{aligned} a_m(V) &= 0.1(V + 40)/(1 - \exp(-(V + 40)/10)), \\ b_m(V) &= 4 \exp(-(V + 65)/18), \\ a_h(V) &= 0.07 \exp(-(V + 65)/20), \\ b_h(V) &= 1/(1 + \exp(-(V + 35)/10)), \\ a_n(V) &= 0.01(V + 55)/(1 - \exp(-(V + 55)/10)), \\ b_n(V) &= 0.125 \exp(-(V + 65)/80), \end{aligned}$$

where $V \in \mathbb{R}$ is the voltage across the membrane, $[m, h, n]^T \in \mathbb{R}^3_{[0,1]}$ is the vector of gating variables which correspond to the state of the membrane's ion channels, $c \in \mathbb{R}^+$ is the constant membrane capacitance, $I_g : \mathbb{R} \times \mathbb{R}^3 \mapsto \mathbb{R}$ is the sum of the membrane currents, and $I : \mathbb{R} \mapsto \mathbb{R}$ is the stimulus current, which when divided by c gives the control input u. $I_b \in \mathbb{R}$ is the baseline current, which represents the effect of other parts of the brain on the neuron under consideration and can be viewed as a bifurcation parameter in the model that controls whether the neuron is in an excitable or an oscillatory regime. The parameters of this model are

$$V_{Na} = 50 \text{ mV},\ V_K = -77 \text{ mV},\ V_L = -54.4 \text{ mV},\ \bar{g}_{Na} = 120 \text{ mS/cm}^2,$$
$$\bar{g}_K = 36 \text{ mS/cm}^2,\ \bar{g}_L = 0.3 \text{ mS/cm}^2,\ I_b = 10\ \mu\text{A/cm}^2,\ c = 1\ \mu\text{F/cm}^2.$$

References

Ashwin P, Swift J (1992) The dynamics of N weakly coupled identical oscillators. J Nonlin Sci 2:69–108

Benabid AL, Pollak P, Gervason C, Hoffmann D, Gao DM, Hommel M, Perret JE, Rougemont JD (1991) Long-term suppression of tremor by chronic stimulation of the ventral intermediate thalamic nucleus. Lancet 337:403–406

Brown E, Holmes P, Moehlis J (2003) Globally coupled oscillator networks. In: Kaplan E, Marsden J, Sreenivasan K (eds) Perspectives and problems in nonlinear science: a celebratory volume in honor of Larry Sirovich. Springer, New York, pp 183–215

Brown E, Moehlis J, Holmes P, Clayton E, Rajkowski J, Aston-Jones G (2004) The influence of spike rate and stimulus duration on noradrenergic neurons. J Comp Neurosci 17:13–29

Brown E, Moehlis J, Holmes P (2004) On the phase reduction and response dynamics of neural oscillator populations. Neural Comp 16:673–715

Cohen A, Holmes P, Rand R (1982) The nature of coupling between segmental oscillators of the lamprey spinal generator for locomotion: a model. J Math Biol 13:345–369

Danzl P, Hespanha J, Moehlis J (2009) Event-based minimum-time control of oscillatory neuron models. Biol Cybern 101:387–399

Danzl P, Nabi A, Moehlis J (2010) Charge-balanced spike timing control for phase models of spiking neurons. Discrete Continuous Dyn Syst Ser A 28:1413–1435

Ermentrout GB (1996) Type I membranes, phase resetting curves, and synchrony. Neural Comp 8:979–1001

Ermentrout GB (2002) Simulating, analyzing, and animating dynamical systems: a guide to XPPAUT for researchers and students. SIAM, Philadelphia

Forger DB, Paydarfar D (2004) Starting, stopping, and resetting biological oscillators: in search of optimal perturbations. J Theor Biol 230:521–532

Gerstner W, Van Hemmen L, Cowan J (1996) What matters in neuronal locking? Neural Comp 8:1653–1676

Ghigliazza RM, Holmes P (2004) A minimal model of a central pattern generator and motoneurons for insect locomotion. SIAM J Appl Dyn Syst 3(4):671–700

Hansel D, Mato G, Meunier C (1993) Phase dynamics for weakly coupled Hodgkin–Huxley neurons. Europhys Lett 25(5):367–372

Hansel D, Mato G, Meunier C (1995) Synchrony in excitatory neural networks. Neural Comp 7:307–337

Hodgkin AL, Huxley AF (1952) A quantitative description of membrane current and its application to conduction and excitation in nerve. J Physiol 117:500–544

Izhikevich EM (2007) Dynamical systems in neuroscience: the geometry of excitability and bursting. MIT Press, London

Keener J, Sneyd J (1998) Mathematical physiology. Springer, New York

Kirk DE (1970) Optimal control theory: an introduction. Dover Publications, USA

Kopell N, Ermentrout G (1990) Phase transitions and other phenomena in chains of coupled oscillators. SIAM J Appl Math 50:1014–1052

Kuramoto Y (1984) Chemical oscillations, waves, and turbulence. Springer, New York

Lenhart S, Workman JT (2007) Optimal control applied to biological models. Chapman and Hall/CRC, London

Merrill D, Bikson M, Jefferys J (2005) Electrical stimulation of excitable tissue: design of efficacious and safe protocols. J Neurosci Methods 141(2):171–198

Moehlis J, Shea-Brown E, Rabitz H (2006) Optimal inputs for phase models of spiking neurons. ASME J Comp Nonlin Dyn 1:358–367

Nabi A, Moehlis J (2009) Charge-balanced optimal inputs for phase models of spiking neurons. In: Proceedings of the 2009 ASME dynamic systems and control conference, Hollywood, DSCC2009-2541

Nabi A, Moehlis J (2010) Nonlinear hybrid control of phase models for coupled oscillators. In: Proceedings of the 2010 American control conference, Baltimore, pp 922–923

Pare D, Curro’Dossi R, Steriade M (1990) Neuronal basis of the Parkinsonian resting tremor: a hypothesis and its implications for treatment. Neuroscience 35:217–226

Revell VL (2005) How to trick mother nature into letting you fly around or stay up all night. J Biol Rhythms 20:353–365

Rinzel J, Ermentrout GB (1998) Analysis of neural excitability and oscillations. In: Koch C, Segev I (eds) Methods in Neuronal Modeling. MIT Press, London, pp 251–291

Rose R, Hindmarsh J (1989) The assembly of ionic currents in a thalamic neuron I. The three-dimensional model. Proc R Soc Lond B 237:267–288

Shaik OS, Sager S, Slaby O, Lebiedz D (2008) Phase tracking and restoration of circadian rhythms by model-based optimal control. Syst Biol IET 2:16–23

Tass PA (1999) Phase resetting in medicine and biology. Springer, New York

Winfree A (2001) The geometry of biological time, 2nd edn. Springer, New York